

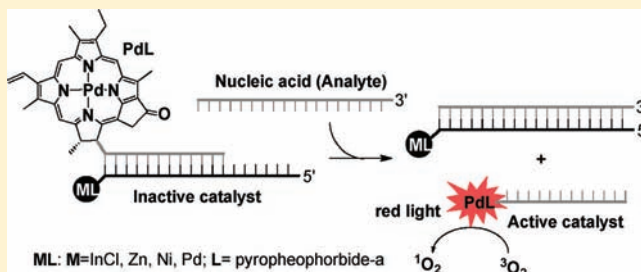
Control of the Photocatalytic Activity of Bimetallic Complexes of Pyropheophorbide-*a* by Nucleic Acids

Dumitru Arian, Larisa Kovbasyuk, and Andriy Mokhir*

Institute of Inorganic Chemistry, Ruprecht-Karls-University of Heidelberg, Im Neuenheimer Feld 270, 69120 Heidelberg, Germany

Supporting Information

ABSTRACT: Photocatalytic activity of a photosensitizer (PS) in an oligodeoxyribonucleotide duplex 5'-PS~ODN1/ODN2~Q-3' is inhibited because of close proximity of a quencher Q. The ODN2 in this duplex is selected to be longer than the ODN1. Therefore, in the presence of a nucleic acid (analyte), which is fully complementary to the ODN2 strand, the duplex is decomposed with formation of an analyte/ODN2~Q duplex and a catalytically active, single stranded PS~ODN1. In this way the catalytic activity of the PS can be controlled by the specific nucleic acids. We applied this reaction earlier for the amplified detection of ribonucleic acids in live cells (Arian, D.; Cló, E.; Gothelf, K.; Mokhir, A. *Chem.—Eur. J.* **2010**, *16*(1), 288). As a photosensitizer (PS) we used In³⁺(pyropheophorbide-*a*)chloride and as a quencher (Q) - Black-Hole-Quencher-3 (BHQ-3). The In³⁺ complex is a highly active photocatalyst in aqueous solution. However, it can coordinate additional ligands containing thiols (e.g., proteins, peptides, and aminoacids), that modulate properties of the complex itself and of the corresponding bio- molecules. These possible interactions can lead to undesired side effects of nucleic acid controlled photocatalysts (PS~ODN1/ODN2~Q) in live cells. In this work we explored the possibility to substitute the In³⁺ complex for those ones of divalent metal ions, Zn²⁺ and Pd²⁺, which exhibit lower or no tendency to coordinate the fifth ligand. We found that one of the compounds tested (Pd(pyropheophorbide-*a*)) is as potent and as stable photosensitizer as its In³⁺ analogue, but does not coordinate additional ligands that makes it more suitable for cellular applications. When the Pd complex was introduced in the duplex PS~ODN1/ODN2~Q as a PS, its photocatalytic activity could be controlled by nucleic acids as efficiently as that of the corresponding In³⁺ complex.



INTRODUCTION

Enzymes are natural catalysts, which have been optimized as the result of billions of years of evolution. They accelerate transformation of molecules with enormous efficiency. Enzymes exhibit their optimal activity in aqueous solutions and usually at physiological pH and temperature. Therefore, enzymatic reactions are applied in analysis for amplification of rare analytes, for example, nucleic acids (polymerase chain reaction, PCR¹) and proteins (enzyme-linked immunosorbent assay, ELISA²).

It is the fundamental challenge for a chemist to develop artificial (chemical) catalysts matching the efficiency of enzymes. Such catalysts can be used, for example, for analyte detection directly in live cells. Enzymes are not well suited for this purpose, since they both do not permeate the cellular membrane and are not stable in the cell because of the intracellular proteolytic activity. We and other research groups have reported a number of nucleic acid dependent, catalytic, chemical reactions, which occur in aqueous solution at mild conditions (≤ 37 °C, pH 6–8).³ Examples include ester hydrolysis catalyzed by imidazole derivatives⁴ or coordinatively unsaturated Cu²⁺ complexes,⁵ Cu⁺ catalyzed alkyne–azide Huisgen cycloaddition (“click” reaction),⁶ Ni²⁺ or Mn²⁺-catalyzed ligation,⁷ several variations of Staudinger reaction,⁸

alkylation⁹ and amide bond-forming reactions,¹⁰ Heck, Wittig, Henry, Michael addition¹¹ and Diels–Alder reactions,¹² Ir⁺-diene catalyzed allylic amination,¹³ a variety of photochemical reactions,¹⁴ and others.³ Several reactions of this type have been applied for detection of endogenous biomolecules (rRNA, mRNA) in live cells.^{8,9,14b} However, despite the significant progress that has been achieved, chemical reactions are still much slower and generate substantially lower number of turnovers than the best enzymatic reactions.^{1,3} This warrants further studies in this field.

We have recently described a new chemical method for detection of nucleic acids in cells based on catalytic photogeneration of ¹O₂.^{14b} The catalyst in this reaction is an oligodeoxyribonucleotide (ODN) duplex consisting of PS~ODN1 and ODN2~Q conjugates, where PS is a photosensitizer (In³⁺(pyropheophorbide-*a*)Cl, InCl-L) and Q is a quencher (Black-Hole-Quencher-3, BHQ-3, Figure 1). In the duplex PS~ODN1/ODN2~Q the photosensitizer is inactive because of quenching of its excited state by the Q. However, in the presence of a nucleic acid (analyte), PS~ODN1/ODN2~Q is converted into an analyte/

Received: July 1, 2011

Published: November 2, 2011

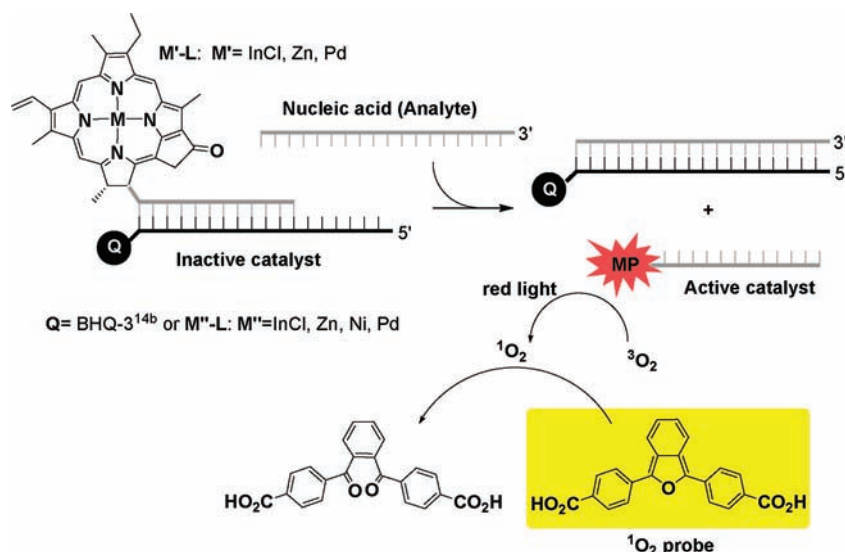
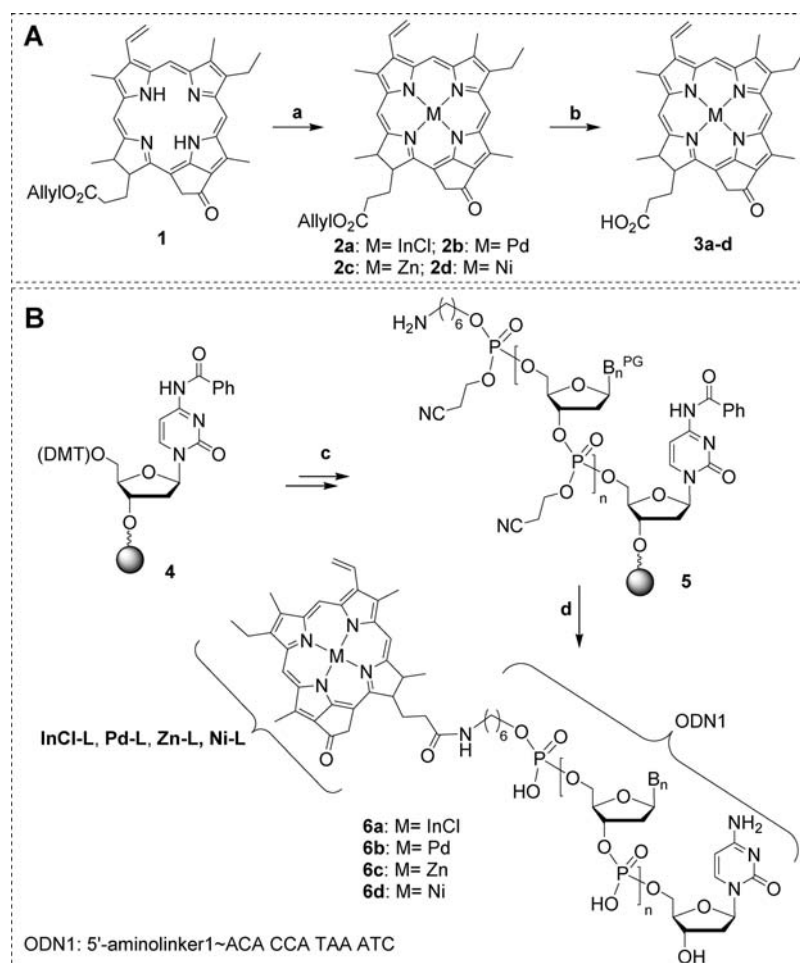


Figure 1. Concept of a fluorogenic and chromogenic assay for amplified detection of nucleic acids based on photocatalytic generation of $^1\text{O}_2$. $M'-L$ is a metal complex ($M' = \text{Zn}^{2+}$, Pd^{2+} , $\text{In}^{3+}\text{-Cl}$) of pyropheophorbide-*a* (*L*): *Q* is a quencher, which is either an organic dye (BHQ-3^{14b}) or a metal complex of pyropheophorbide-*a* ($M'' = \text{Zn}^{2+}$, Ni^{2+} , Pd^{2+} , $\text{In}^{3+}\text{-Cl}$).

Scheme 1. Synthesis of $M(\text{pyropheophorbide-}a)$, Where $M = \text{Pd}^{2+}$, Zn^{2+} , and Ni^{2+} (A) and Their 5'-Conjugates with ODN1 Strand ($M'-L \sim \text{ODN1}$, B)



A: synthesis of **3a** ($M = \text{In}^{3+}\text{Cl}$) was described elsewhere^{14b} (a) for $M = \text{Zn}^{2+}$, Ni^{2+} : MCl_2 , DMF; for $M = \text{Pd}^{2+}$: $\text{Pd}(\text{OAc})_2$, MeOH; (b) $[\text{Pd}(\text{PPh}_3)_4]$, PPh_3 , $(\text{NH}_2\text{Et}_2)(\text{HCO}_3)$, CH_2Cl_2 . **B:** (c) 1. ODN1 was compiled on a DNA/RNA synthesizer; the last step was a coupling of 5'-MMT-Amino-Modifier C6-CE; 2.1 % TFA in CH_2Cl_2 ; (d) 1. Metal complex (**3a-d**), HBTU, HOBT, DIEA, DMF; 2. NH_3 (27% in water).

ODN2~Q duplex and a catalytically active PS~ODN1. The latter compound acts as an efficient photosensitizer: 1 equiv of PS~ODN1 catalyzes the photogeneration of over 6000 equiv of $^1\text{O}_2$. $^1\text{O}_2$ released in this reaction bleaches 1,3-di(4-carboxyphenyl)isobenzofuran that can be detected by using either UV-visible or fluorescence spectroscopy.^{14b} InCl-L is a highly active photosensitizer in aqueous solution. However, the chloride ligand in this complex can be potentially substituted for thiol groups containing, for example, proteins, peptides, and aminoacids. This interaction is expected to modulate properties of both the complex and the corresponding biomolecule that can cause undesired side effects of the catalyst in cells.

Herein we report PS~ODN1/ODN2~Q duplexes, in which In^{3+} was substituted for divalent metal ions, Zn^{2+} and Pd^{2+} , whose complexes exhibit low or no tendency to coordinate the fifth ligand.

Furthermore, we tested complexes of pyropheophorbide-*a* with In^{3+} , Pd^{2+} , Zn^{2+} , Ni^{2+} as quenchers (Q). Overall, nine ODN duplexes, where both a photosensitizer and a quencher are metal complexes ($\text{M}'\text{-L}\sim\text{ODN1}/\text{ODN2}\sim\text{M}''\text{-L}$, Figure 1), were prepared by self-assembly. In these duplexes homo- and heterobimetallic complexes with $\text{M}'/\text{M}'' = \text{In}^{3+}/\text{Zn}^{2+}$, $\text{In}^{3+}/\text{Pd}^{2+}$, $\text{In}^{3+}/\text{Ni}^{2+}$, $\text{Zn}^{2+}/\text{Pd}^{2+}$, $\text{Zn}^{2+}/\text{Ni}^{2+}$, $\text{Pd}^{2+}/\text{Ni}^{2+}$, $\text{In}^{3+}/\text{In}^{3+}$, $\text{Zn}^{2+}/\text{Zn}^{2+}$, $\text{Pd}^{2+}/\text{Pd}^{2+}$ are present. Interaction of the metal containing units ($\text{M}'\text{-L}\sim\text{M}''\text{-L}$) with each other in $\text{M}'\text{-L}\sim\text{ODN1}/\text{ODN2}\sim\text{M}''\text{-L}$ duplexes and their DNA-induced dissociation/activation was studied by using UV-visible and fluorescence spectroscopy. Several nucleic acid stabilized, homo- (Zn^{15} and Ni^{16}) and heterobimetallic (Zn/Ni^{17}) porphyrinates have been prepared before in the framework of studies toward the dyes with tunable optical properties. However, catalytic properties of these compounds have not been explored yet. In this work we realized for the first time the control of the catalytic activity of artificial bimetallic complexes by a representative biomolecule (nucleic acid).

RESULTS AND DISCUSSION

Synthesis of PS~ODN1 and ODN2~Q Conjugates.

In(pyropheophorbide-*a*)Cl (complex 3a) was prepared as described previously.^{14b} Pd^{2+} complex 3b was prepared in two steps (Scheme 1A). First, allyl ester of Pd-(pyropheophorbide-*a*) (2b) was obtained with 32% yield from $\text{Pd}(\text{OAc})_2$ and allyl ester of pyropheophorbide-*a* suspended in $\text{CHCl}_3/\text{MeOH}$ mixture. Low yield of this complex was due to Pd^{2+} -induced decomposition of the ligand. Next, allyl ester of Pd(pyropheophorbide-*a*) was deprotected in the presence of $[\text{Pd}(\text{PPh}_3)_4]$ catalyst. The resulting Pd-(pyropheophorbide-*a*) complex (3b) contains a free carboxylic acid group, which is suitable for conjugation with ODNs. Synthesis of the corresponding Pt^{2+} complex by using this and other known methods was not successful. Complexes of Zn^{2+} and Ni^{2+} (3c, 3d) were obtained analogously to 3b, except that in the first step MCl_2 salts and dimethylformamide (DMF) were used in place of a correspondingly $\text{Pd}(\text{OAc})_2$ and $\text{CHCl}_3/\text{MeOH}$ mixture.

5'-Modified ODNs ($\text{M}'\text{-L}\sim\text{ODN1}$) were synthesized in accordance to Scheme 1B. First, an ODN strand was compiled on a controlled pore glass (CPG) solid support under standard conditions of DNA synthesis using a DNA/RNA synthesizer. Commercially available 5'-MMT-Amino-Modifier C6-CE phosphoramidite was coupled in the last step to introduce a terminal primary amino group protected with a 4-monomethoxytrityl (MMT) fragment. Next, the protection was removed under

acidic conditions and complexes 3a–d were coupled in the presence of O-benzotriazole-*N,N,N',N'*-tetramethyluronium-hexafluorophosphate (HBTU) activator. The resulting conjugates were cleaved and deprotected by their treatment with concentrated aqueous ammonia solution and purified by HPLC. Purity of the resulting compounds was confirmed by analytical HPLC, and their identity by MALDI-TOF mass spectrometry.

An HPLC profile and a MALDI-TOF mass spectrum of a representative conjugate (6b) are shown in Figure 2.

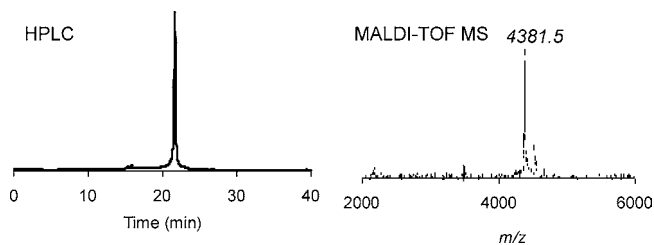
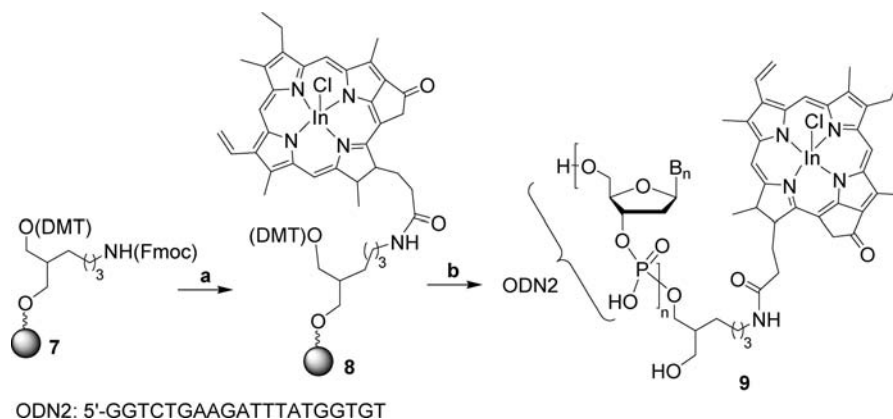


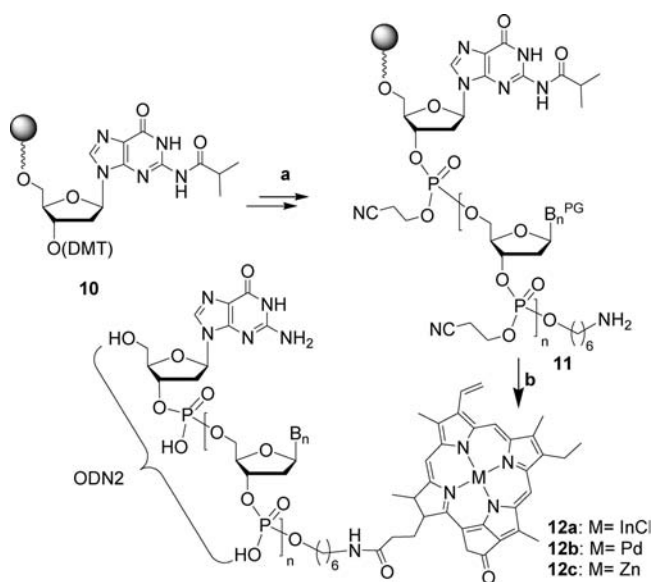
Figure 2. Representative HPLC profile (solvent A: $(\text{NEt}_3\text{H})(\text{OAc})$, 0.1 M in water; solvent B: CH_3CN ; gradient: 5 min washing with solvent A; solvent B content is increased from 0 to 90% within 30 min.) and a MALDI-TOF mass spectrum of ODN conjugate 6b containing Pd^{2+} (pyropheophorbide-*a*) 3b.

We first attempted to prepare 3'-modified ODNs ($\text{ODN2}\sim\text{M}''\text{-L}$) by the method previously described for synthesis of $\text{ODN}\sim\text{L}\sim\text{InCl}\text{-}3'$ conjugates (Scheme 2).^{14b} In particular, as a starting point we used commercially available solid support 7, which contains an Fmoc-protected, aliphatic, primary amino group and a DMT-protected, primary alcohol group (Scheme 2). The Fmoc group was deprotected by piperidine/DMF mixture and complexes 3a–d were coupled as described above. Next, the DMT-group was cleaved and the ODN strand was synthesized on a DNA/RNA synthesizer. Following cleavage and deprotection with concentrated ammonia, we analyzed the reaction mixtures by HPLC and MALDI-TOF mass spectrometry. We observed that in all cases except of the indium complex the conjugate $\text{ODN2}\sim\text{L}\text{-}3'$ rather than the expected $\text{ODN2}\sim\text{M}''\text{-L}$ ($\text{M} = \text{Pd}, \text{Zn}, \text{Ni}$) was formed. These data indicated that the complexes of Pd, Zn, and Ni were not stable at the conditions of DNA synthesis. In the model experiments with complexes 3b–d, we confirmed that the demetalation occurred during the repeating steps of DMT-group deprotection under acidic conditions. To avoid the acidic treatment, we applied an alternative synthetic approach outlined in Scheme 3. In particular, 3'-amino-modified ODN 11 was first prepared by so-called reverse DNA synthesis. Then complexes 3a, 3b, and 3c were coupled to 11 in the presence of HBTU, and the resulting intact metal complex containing conjugates were worked out and purified as described above. An HPLC profile and a MALDI-TOF mass spectrum of a representative pure conjugate (12b) obtained by this method are shown in Figure 3. Metal complex-containing conjugates are not ionized so easily as unmodified oligonucleotides. Therefore, high laser energy is required to get the signal in MALDI-TOF mass spectra. In this case MALDI-TOF mass spectra are used only for identification of the conjugates, whereas their purity is determined by analytical HPLC. Concentration of the conjugates was determined from absorbance of their solutions at 260 nm. Extinction coefficient of the conjugates was calculated by summing up the extinction coefficients of

Scheme 2. Synthesis of 3'-Modified Conjugates of ODN2 with In^{3+} (pyropheophorbide-*a*)Cl (3a)

(a) 1. piperidine, DMF; 2. complex 3a, HBTU, HOBT, DIEA, DMF; (b) 1. synthesis of ODN2 on a DNA/RNA synthesizer; 2. NH_3 (27% in water).

Scheme 3. Synthesis of 3'-Modified Conjugates of ODN2 with Acid Sensitive Metal Complexes



(a) 1. ODN2 was compiled on a DNA/RNA synthesizer under conditions of reverse (5'→3') DNA synthesis; the last step was coupling of 5'-MMT-Amino-Modifier C6-CE; 2. 1% TFA in CH_2Cl_2 ; (b) 1. Metal complex (3b, 3c), HBTU, HOBT, DIEA, DMF; 2. NH_3 (27% in water).

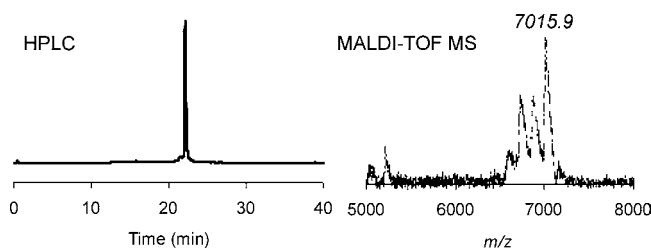


Figure 3. Representative HPLC profile (solvent A: $(\text{NEt}_3\text{H})\text{OAc}$, 0.1 M in water; solvent B: CH_3CN ; gradient: 5 min washing with solvent A; solvent B content is increased from 0 to 90% within 30 min.) and a MALDI-TOF mass spectrum of ODN conjugate 12b containing Pd^{2+} (pyropheophorbide-*a*).

individual nucleotides and of corresponding chemical modifiers (L/(mol cm)): $\epsilon_{260}(\text{InCl-L}) = 12000$; $\epsilon_{260}(\text{Pd-L}) = 15000$; $\epsilon_{260}(\text{Zn-L}) = 11000$; $\epsilon_{260}(\text{Ni-L}) = 10000$.

Binding of Axial Ligands to Metal Ions in $\text{M}'\text{-L}\sim\text{ODN1}$ Conjugates. Next, we studied coordination of 1-thionaphthol (RSH) to metal ions in $\text{M}'\text{-L}\sim\text{ODN1}$ conjugates. This ligand models naturally occurring thiols and, because of its aromatic rest, causes strong quenching of the fluorescence of $\text{M}'\text{-L}$ complexes upon the coordination. Thus, formation of $\text{M}'(\text{SR})\text{-L}$ associates can be conveniently monitored by using fluorescence spectroscopy. Conjugates 6a–c were titrated with increasing concentrations of RSH in phosphate buffer (pH 7.0), and the fluorescence intensity of the resulting solutions was monitored. We observed that the fluorescence of $\text{InCl-L}\sim\text{ODN1}$ (6a) was affected by the ligand, whereas the one of $\text{Pd-L}\sim\text{ODN1}$ (6b) and $\text{Zn-L}\sim\text{ODN1}$ (6c) stayed practically unchanged (Figure 4). These data indicate that RSH

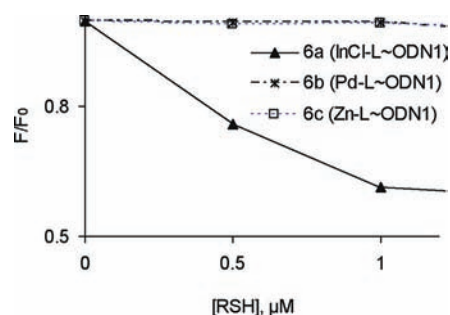


Figure 4. Fluorescent titration of 6a–c (1 μM) with 1-thionaphthol (RSH) in phosphate buffer (100 mM, pH 7.0); $\lambda_{\text{ex}} = 430$ nm; $\lambda_{\text{em}} = 660$ nm; titration curves for 6b and 6c are overlapping with each other; the titrations were repeated three times; standard deviations of the fluorescence intensities measured do not exceed 8%.

binds to the In complex and does not bind to the Pd and Zn complexes.

We also investigated binding of *N*-(9-fluorenylmethoxycarbonyl)cystein (Fmoc-Cys) to conjugates 6a and 6b. The Fmoc-Cys ligand is a better model of naturally occurring thiols than 1-thionaphthol, since it contains the aliphatic CH_2SH fragment, which is also found in cystein and glutathione. In contrast, the SH-group in 1-thionaphthol is

substantially more acidic than that one in cystein and glutathione. Titration of conjugates **6a** and **6c** with Fmoc-Cys leads to analogous, but less pronounced effects: fluorescence of the In-complex is quenched and that of the Pd-complex is not quenched (Supporting Information, Figure S3). Both data sets described confirm that, in contrast to the InCl-L complex, the corresponding Pd-complex exhibits substantially lower affinity toward additional thiol containing ligands in aqueous solution. Thus, the Pd complex is expected to be better suited for cellular applications than the corresponding In complex.

Photocatalytic Properties of Metal Complexes of Pyropheophorbide-*a* Conjugated to ODNs. Photogeneration of $^1\text{O}_2$ in the presence of complex~ODN conjugates and upon exposure to red light (650 nm) was monitored by using 1,3-di(4-carboxyphenyl)isobenzofurane as a $^1\text{O}_2$ -trap. In particular, the latter compound is yellow. It reacts with $^1\text{O}_2$ with formation of [2 + 4] addition product, which spontaneously decomposes with formation of the colorless product (Figure 1).

Among four complexes studied only InCl-L (conjugates **6a**, **12a**) and Pd-L (conjugates **6b**, **12b**) exhibit strong photosensitizing properties at physiological conditions, whereas Zn-L (conjugates **6c**, **12c**) is substantially less effective and Ni-L (conjugate **6d**) is not active at all (Figure 5).

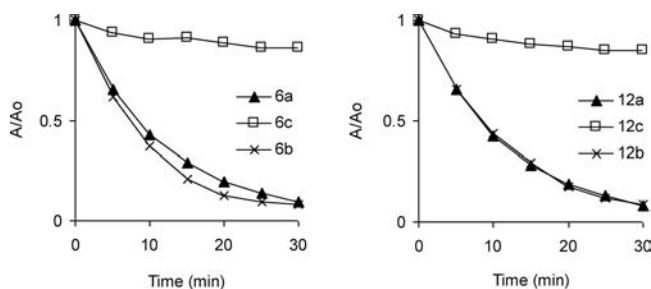


Figure 5. Cleavage of 1,3-di(4-carboxyphenyl)isobenzofurane (100 μM) in the presence of **6a**–**c** and **12a**–**c** (300 nM); buffer: phosphate (100 mM, pH 7.0); mixtures were exposed to light (660 nm); absorbance at 460 nm (*A*) was measured at different exposure times. A_0 is absorbance of the mixtures before their exposure to light; the titrations were repeated 3 times; standard deviations of the absorbance values measured do not exceed 5%.

The latter effect is not surprising, since it is known that Ni^{2+} inhibits the photosensitizing properties of tetrapyrrole ligands, whereas it is generally not the case for Zn^{2+} ion.¹⁸ Interestingly, the activity of both Pd-L and InCl-L complexes is independent from the sequence of ODNs to which they are conjugated. In particular, two types of conjugates carrying the same photosensitizer and containing either a short ODN strand (12-mer, **6a**, **6b**) or a long G-rich strand (20-mer, **12a**, **12b**) exhibit practically the same activity (Figure 5).

A nucleic acid controlled photocatalyst is expected to generate many equivalents of $^1\text{O}_2$ from $^3\text{O}_2$ upon its exposure to light. This reaction amplifies nucleic acids that should allow detecting rare nucleic acids in cells. $^1\text{O}_2$ and other reactive species generated in this process react not only with $^1\text{O}_2$ probes as it is outlined in Figure 1, but can also attack the photocatalyst itself inducing its bleaching. This side reaction reduces the amplification factor. Therefore, we studied the photostability of the metal complexes in the conjugates to evaluate them as potential catalysts (Figures 1, 6).

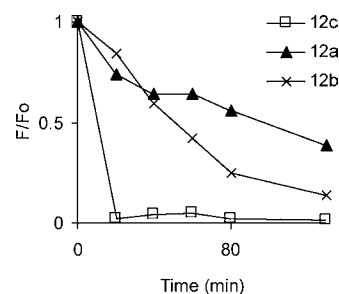


Figure 6. Photostability of the complexes in **12a**, **12b**, **12c**. The conjugates (5 μM) were irradiated with light (635 nm laser with 2.6 mW power) in phosphate buffer (100 mM, pH 7); fluorescence ($\lambda_{\text{ex}} = 430$ nm; $\lambda_{\text{em}} = 670$ nm) of nonirradiated conjugates is F_0 and that of irradiated samples is F ; the titrations were repeated 3 times; standard deviations of the fluorescence intensities do not exceed 11%.

In particular, we observed that Pd-L in conjugate **12b** is practically as stable as InCl-L in **12a**, whereas Zn-L in **12c** is degraded very quickly at the same experimental conditions. These data indicate that poor performance of the Zn-L as a photocatalyst of $^1\text{O}_2$ generation can be explained by its low photostability (Figure 5, 6).

Hybridization-Induced Formation of Bimetallic Complexes of Pyropheophorbide-*a*. Binding of conjugates containing InCl-L (**6a**, **12a**), Pd-L (**6b**, **12b**), Zn-L (**6c**, **12c**), and Ni-L (**6d**) to each other with formation of homo- and heterobimetallic complexes (Figure 1, Table 1) was monitored

Table 1. Spectral Changes upon Formation of Bimetallic Complexes from $\text{M}'\text{-L}\sim\text{ODN1}$ and $\text{ODN2}\sim\text{L-M}''$

entry	$\text{M}'\text{-L}\sim\text{ODN1}/\text{ODN2}\sim\text{M}''\text{-L}$ (M'/M'') ^a	fluorescence: $F_{\text{M}'\text{M}''}/(F_{\text{M}'} + F_{\text{M}''})$		absorbance: $A_{\text{M}'\text{M}''}/(A_{\text{M}'} + A_{\text{M}''})$ ^c	
		-DNA ^d	+DNA	-DNA	+DNA
1	6a/12a (In/In)	0.22	0.90	0.50	0.85
2	6a/12b (In/Pd)	0.26			
3	6a/12c (In/Zn)	0.30			
4	6d/12a (Ni/In)	0.11	0.90	0.56	0.94
5	6b/12b (Pd/Pd)	0.23	0.85	0.57	0.80
6	6b/12c (Pd/Zn)	0.09			
7	6d/12b (Ni/Pd)	0.35	0.90	0.64	0.88
8	6c/12c (Zn/Zn)	0.14			
9	6d/12c (Ni/Zn)	0.15			

^aBuffer, 100 mM phosphate, pH 7.0; L, pyropheophorbide-*a*. ^b $F_{\text{M}'\text{M}''}$, fluorescence intensity of the duplex built of $\text{M}'\text{-L}\sim\text{ODN1}$ and $\text{ODN2}\sim\text{L-M}''$; $\lambda_{\text{ex}} = 430$ nm, $\lambda_{\text{em}} = 670$ nm; $F_{\text{M}'}$ and $F_{\text{M}''}$ are fluorescence intensities of solutions containing either $\text{M}'\text{-L}\sim\text{ODN1}$ or $\text{ODN2}\sim\text{L-M}''$ (each 0.5 μM), correspondingly; [DNA] = 0.5 μM . ^c $A_{\text{M}'\text{M}''}$, $A_{\text{M}'}$ and $A_{\text{M}''}$ are absorbances at 660 nm of the duplex, strands $\text{M}'\text{-L}\sim\text{ODN1}$ and $\text{ODN2}\sim\text{L-M}''$ (each 2 μM), correspondingly; [DNA] = 2 μM . ^dDNA sequence: 5'-CGC ACC ATA AAT CTT CAG ACC.

by using fluorescence and UV-visible spectroscopy (Figure 7). The fluorescence of the dyes is quenched down to 9–35% of the initial fluorescence upon formation of the bimetallic complexes, whereas the absorbance intensity at 660 nm is reduced by ~1.6–2 fold (Table 1). Analogous fluorescence quenching and reduction of intensity of Soret and Q-bands of the dyes have been observed by other research groups, which

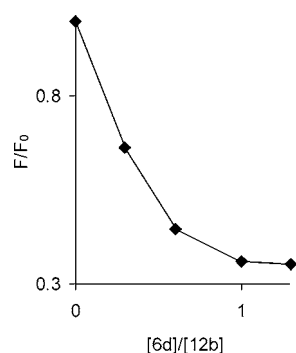


Figure 7. Titration of conjugate **12b** ($0.5 \mu\text{M}$) with conjugate **6d** in phosphate buffer (100 mM , $\text{pH } 7.0$); F is fluorescence intensity; $\lambda_{\text{ex}} = 430 \text{ nm}$; $\lambda_{\text{em}} = 670 \text{ nm}$; F_0 is fluorescence intensity of **12b** ($0.5 \mu\text{M}$) before addition of **6d**; the titrations were repeated three times; standard deviations of the fluorescence intensities measured do not exceed 8%.

studied formation of dimers of porphyrins and their zinc complexes.^{16,17,19}

The fact that the absorbance of the bimetallic complexes is not equal to the sum of absorbances of the corresponding monomers indicates that the dyes are interacting with each other in the ground state. It is sensible to suggest that the complexes are held together by π - π interactions forming homo- and heterobimetallic complexes $\text{M}'\text{-L}/\text{M}''\text{-L}$ on the terminus of ODN duplexes. Correspondingly, the quenching observed in the fluorescence spectra of these duplexes occurs mainly via the contact mechanism. By using the fluorescent titrations (as shown in Figure 7 for **6d/12b** complex) we found that the stoichiometry of all 9 possible bimetallic complexes ($\text{In}^{3+}/\text{Zn}^{2+}$, $\text{In}^{3+}/\text{Pd}^{2+}$, $\text{In}^{3+}/\text{Ni}^{2+}$, $\text{Zn}^{2+}/\text{Pd}^{2+}$, $\text{Zn}^{2+}/\text{Ni}^{2+}$, $\text{Pd}^{2+}/\text{Ni}^{2+}$, $\text{In}^{3+}/\text{In}^{3+}$, $\text{Zn}^{2+}/\text{Zn}^{2+}$, $\text{Pd}^{2+}/\text{Pd}^{2+}$) is 1:1. The fluorescence intensity of the bimetallic complexes is increased linearly in the concentration range between 0.2 and $1 \mu\text{M}$, whereas at $\geq 1 \mu\text{M}$ we observed slight deviations from the linearity. These data indicate that the complexes exist as monomers at $\leq 1 \mu\text{M}$ and start aggregating at $\geq 1 \mu\text{M}$.

Nucleic Acid Controlled Photocatalysts. We observed that the bimetallic complexes in duplexes $\text{M}'\text{-L}\sim\text{ODN1}/\text{ODN2}\sim\text{L}\text{-M}''$ are poor photosensitizers in comparison with their monometallic constituents (Table 2). The strong effect was observed in pairs $\text{Ni-L}/\text{InCl-L}$ and $\text{Ni-L}/\text{Pd-L}$ in duplexes **6d/12a** and **6d/12b** correspondingly. In particular, monometallic InCl-L complex in **12a** ($0.3 \mu\text{M}$) catalyzes photocleavage of 1,3-di-(4-carboxyphenyl)isobenzofurane⁴ with the rate of $20.6 \mu\text{M}/\text{min}$, whereas the same complex in the **6d/12a** duplex is 6 times less active. Analogously, Pd-L complex in **6d/12b** is 5 times less active than the same photosensitizer in single stranded **12b**. It should be noted that organic dye **BHQ-3** quenches both InCl-L and Pd-L substantially stronger: 30-fold.^{14b}

We selected the ODN2 sequence (20-mer) in conjugates **12a-c** to be longer than the ODN1 sequence (11-mer) of conjugates **6a-d**. Therefore, addition of analyte nucleic acid (21-mer), which is fully complementary to the ODN2, leads to quick (within 15 min) and complete conversion of duplexes **6/12** into single stranded conjugates **6** and duplexes **12/analyte**. In this case the interaction between the terminal modifications of **6a-d** and **12a-c** is expected to be disrupted. Indeed, we observed that addition of the analyte DNA to representative duplexes **6a/12a**, **6d/12a**, **6b/12b**, and **6d/12b** (entries 1, 4, 5,

Table 2. Nucleic Acid Dependent Photosensitizing Properties of Bimetallic Complexes in $\text{M}'\text{-L}\sim\text{ODN1}/\text{ODN2}\sim\text{L}\text{-M}''$ Duplexes

entry	$\text{M}'\text{-L}\sim\text{ODN1}/\text{ODN2}\sim\text{L}\text{-M}''$ (M'/M'')	rate of photodecomposition of $^1\text{O}_2\text{-trap}^a$	
		-DNA ^c	+DNA
1	6a (In)	20.6 ± 1.4	
2	9a (In)	20.6 ± 3.1	
3	6a/12a (In/In) ^b	4.3 ± 2.6	
4	6a/12b (In/Pd) ^b	9.2 ± 2.4	
5	6d/12a (Ni/In)	3.4 ± 1.0	12.0 ± 1.8
6	6b (Pd)	23.2 ± 3.1	
7	12b (Pd)	20.7 ± 1.5	
8	6b/12b (Pd/Pd) ^b	9.9 ± 2.0	
9	6d/12b (Ni/Pd)	4.0 ± 2.1	12.0 ± 3.2

^aInitial decomposition rate: $v_0 = -(dc/dt)_0$ ($\mu\text{M}/\text{min}$) (determined in the linear region of $<30\%$ conversion of the $^1\text{O}_2\text{-trap}$), where c is concentration of the $^1\text{O}_2\text{-trap}$: 1,3-di-(4-carboxyphenyl)-isobenzofurane; conditions: conjugate concentrations $\sim 0.3 \mu\text{M}$; initial concentration of the $^1\text{O}_2\text{-trap}$ $c_0 = 300 \mu\text{M}$; buffer, phosphate, 100 mM , $\text{pH } 7.0$; light source, LED-array: 660 nm . ^bTotal concentration of the photosensitizers ($\text{M}'\text{-L}$, $\text{M}''\text{-L}$) was kept at $0.3 \mu\text{M}$. ^cDNA sequence: 5'-CGC ACC ATA AAT CTT CAG ACC.

7) restores the fluorescence of complexes InCl-L and Pd-L (Table 1). Expected changes are also observed in UV-visible spectra. In particular, intensities of the peaks corresponding to $\text{M}'\text{-L}$ and $\text{M}''\text{-L}$ chromophores ($640\text{--}680 \text{ nm}$) are increased in the presence of the analyte DNA (Table 1). We observed that the nucleic acid induced disruption of the bimetallic complexes leads to about 60% recovery of the photosensitizing activity of the dyes (entries 5 and 9, Table 2). The incomplete recovery can be explained by the intermolecular interactions of the photosensitizers (InCl-L and Pd-L) and the quencher (Ni-L) in solution.

CONCLUSIONS

We generated a series of individual homo- and heterobimetallic complexes at low concentrations ($\leq 1 \mu\text{M}$) and at a physiologically relevant pH. The photocatalytic activity of these complexes is significantly lower than the activity of the monometallic analogues. We demonstrated for the first time that the functional properties (catalytic activity) of the artificial homo- and heterobimetallic complexes can be controlled by a representative biomolecule (nucleic acids). Finally, we have substituted In^{3+} for Pd^{2+} to obtain the photosensitizer $\text{Pd-L}\sim\text{ODN1}$, which exhibits photocatalytic properties similar to those of $\text{InCl-L}\sim\text{ODN1}$, but does not react with thiol containing ligands at micromolar concentrations. Therefore, the new Pd-analogue is expected to exhibit fewer undesired side effects when applied in cells.

In future studies we will further optimize the efficiency of quenching of the catalyst in the deactivated complex, improve the sensitivity of this photocatalyst, and approach the problem of its cell membrane permeability by using chemically modified oligonucleotides as nucleic acid recognition elements, for example, phosphorothioate DNAs or LNAs.

EXPERIMENTAL SECTION

Commercially available chemicals of the best quality from Aldrich/Sigma/Fluka (Germany) were obtained and used without purification. Phosphoramidites and controlled pore glass (CPG) solid support were

from Glen Research (U.S.A.) and Link Technologies (U.K.). MALDI-TOF mass spectra were recorded on a Bruker BIFLEX III spectrometer. The matrix mixture (2:1 v/v) was prepared from 6-aza-2-thiothymine (ATT, saturated solution in acetonitrile) and diammonium citrate (0.1 M in water). Samples for mass spectrometry were prepared by the dried-droplet method by using a 1:2 probe/matrix ratio. Mass accuracy with external calibration was 0.1% of the peak mass, that is, ± 7.0 at m/z 7000. HPLC was performed at 22 °C on a Shimadzu liquid chromatograph equipped with a UV detector and a Macherey–Nagel Nucleosil C4 250 \times 4.6 mm column. HPLC gradient, (solution A: 0.1 M (NEt₃H)(OAc), solution B: CH₃CN): from 0 to 90% in 30 min. UV/vis spectra were measured on a Varian Cary 100 Bio UV/vis spectrophotometer by using 1 cm optical path black-wall absorption semimicrocuvettes (Hellma GmbH, Germany) with a sample volume of 0.7 mL. These cuvettes were also used for photochemical experiments. Light from different light sources was applied from the top of the cuvette via an optical fiber. Fluorescence spectra were acquired on a Varian Cary Eclipse fluorescence spectrophotometer by using black-wall fluorescence semimicrocuvettes (Hellma GmbH, Germany) with a sample volume of 0.7 mL.

Synthesis of Metal Complexes of Pyropheophorbide-

a. Allyl Ester of Ni²⁺(pyropheophorbide-a) (2d). A mixture of anhydrous NiCl₂ (50 mg; 390 μ mol) and allyl ester of pyropheophorbide-a (10 mg; 17.4 μ mol) in DMF (10 mL) was purged with argon and heated to 140 °C. It was kept at these conditions in the dark for 30 min. After the reaction completion (TLC monitoring), the solvent was evaporated and the residue was purified by column chromatography using as an eluent a mixture of EtOAc and DCM (1:10). Yield is 10 mg (93%). TLC: R_f (EtOAc/DCM 1:15) = 0.36; for comparison, the ligand has R_f = 0.52 at these conditions. LDI-TOF MS: m/z calcd. for C₃₆H₃₆N₄NiO₃ [M+e⁻]⁻: 630.2; found: 630.4

Ni²⁺(pyropheophorbide-a) (3d). [Pd(PPh₃)₄] (4.3 mg, 3.6 μ mol) and PPh₃ (0.6 mg, 2.2 μ mol) in CH₂Cl₂ (1 mL) were added to a suspension containing Ni²⁺(pyropheophorbide-a allyl ester) (10.2 mg, 16.2 μ mol) and (NH₂Et)₂(HCO₃) (12.7 mg, 94 μ mol) in CH₂Cl₂ (5 mL). The resulting suspension was stirred until complete conversion of the starting material was achieved (~15 min; the reaction was monitored by TLC). The resultant solution was directly loaded onto a chromatography column and eluted with 5% methanol, 0.1% AcOH in DCM. Free acid **3d** was obtained in 92% yield (8.8 mg). TLC: R_f = 0.49 (5% methanol, 0.1% AcOH in DCM). LDI TOF MS: m/z calcd. for C₃₃H₃₂N₄NiO₃ [M+1e⁻]⁻: 590.2; found: 590.3. UV-visible absorbance spectrum in methanol: λ_{\max} (Log ϵ) = 650 (4.5), 420 (4.5), 397 nm (4.5).

Allyl Ester of Zn²⁺(pyropheophorbide-a) (2c). Complex **2c** was obtained analogously to **2d** except that ZnCl₂ was used in place of NiCl₂. The synthesis was conducted on a larger scale: ZnCl₂ (100 mg; 0.740 mmol), allyl ester of pyropheophorbide-a (23 mg; 40 μ mol), DMF (15 mL). Complex **2c** was obtained with 75% yield. TLC: R_f (EtOAc/DCM 1:15) = 0.41. LDI TOF MS: m/z calcd. for C₃₆H₃₆N₄O₃Zn [M+e⁻]⁻: 636.2; found: 636.4.

Zn²⁺(pyropheophorbide-a) (3c). Complex **3c** was obtained from **2c** analogously to synthesis of **3d** described above. Yield of **3c** was 70% yield. TLC: R_f = 0.42 (5% methanol, 0.1% AcOH in DCM). LDI TOF MS: m/z calcd. for C₃₃H₃₂N₄O₃Zn [M+e⁻]⁻: 596.2; found: 596.3. UV-visible absorbance spectrum in methanol: λ_{\max} (Log ϵ) = 659 (4.5), 430 (4.6), 411 nm (4.5).

Allyl Ester of Pd²⁺(pyropheophorbide-a) (2b). Allyl ester of pyropheophorbide-a (5.2 mg; 9 μ mol) was dissolved in CHCl₃ (20 mL), and Pd(OAc)₂ (50 mg) suspended in MeOH (10 mL) was added. The resulting mixture was purged with argon. After stirring overnight at 22 °C, aqueous solution of NaHCO₃ (4%, 20 mL) was added, and the reaction mixture was stirred for 20 min. Then the mixture was filtered and the filtrate was washed with water. The organic phase was separated and dried over Na₂SO₄. After filtration of Na₂SO₄, the solvents were removed, and the residue was purified by column chromatography using 10% EtOAc in DCM as an eluent. Yield of **2b** was 2.0 mg (32%). TLC: R_f (EtOAc/DCM 1:15) = 0.43. LDI TOF MS: m/z calcd. for C₃₆H₃₆N₄O₃Pd [M+e⁻]⁻: 678.2; found: 678.3.

Pd²⁺(pyropheophorbide-a) (3b). Complex **3b** was obtained from **2b** analogously to the synthesis of **3d** described above. Yield of **3b** was 85%. TLC: R_f = 0.47 (5% methanol, 0.1% AcOH in DCM). LDI TOF MS: m/z calcd. for C₃₃H₃₂N₄O₃Pd [M+1e⁻]⁻: 638.2; found: 638.3. UV-visible absorbance spectrum in methanol: λ_{\max} (Log ϵ) = 641 (4.6), 420 (4.5), 395 nm (4.5).

Synthesis of P1~ODN1 Conjugates. Oligodeoxyribonucleotides (ODNs) were prepared using either standard (3'→5') or reversed (5'→3') synthesis on a DNA/RNA synthesizer. Commercially available phosphoramidites (dT-CE, Bz-dC-CE, Bz-dA-CE, dmF-dG-CE, 5'-MMT-Amino-Modifier C6-CE) and solid supports (Bz-dC SynBase controlled pore glass (CPG), 3'-Amino-Modifier C7 CPG) were used in the 3'→5' synthesis (Link Technologies, Scotland). 3'-DMT-protected 5'-phosphoramidites (dT-5'-CE, Bz-dC-5'-CE, Bz-dA-5'-CE and dmF-dG-5'-CE) and the corresponding solid support (dG-5'-SynBase CPG, Link Technologies, Scotland) were used in the reversed (5'→3') synthesis. ODNs were cleaved from the solid support and deprotected by the treatment with aqueous NH₃ solution (27%) at 55 °C for 2 h. Crude ODNs were purified by reversed phase HPLC. Purity of the conjugates was confirmed by analytical HPLC and their identity by MALDI-TOF mass spectrometry (Supporting Information, Figures S1–S3).

General Procedure for Cleavage of MMT-Group (Step c.2 in Scheme 1 and Step a.2 in Scheme 3). 4-Monomethoxytrityl (MMT) protected amino~ODN~CPGs (1 μ mol scale synthesis) were deprotected by their treatment with 1% trifluoroacetic acid (TFA) in CH₂Cl₂ (1 mL) for 3 min. Then samples were washed with 1% TFA in CH₂Cl₂ (2 \times 2 mL) and CH₂Cl₂ (3 \times 2 mL), and dried at 0.01 mbar pressure for 1 h.

Cleavage of Fmoc-Group (Step a.1 in Scheme 2). Solid support **7** containing and amino group protected with fluorenylmethoxycarbonyl (Fmoc) group (1 μ mol of the Fmoc-group on the solid support) was treated with piperidine/DMF (4/1) mixture for 40 min. Then the solid support was washed with DMF (3 \times 2 mL), CH₃CN (3 \times 2 mL) and dried at 0.01 mbar pressure for 1 h.

Coupling of Metal Complexes on Amino Modified ODNs. Metal complex containing a carboxylic acid fragment (10 μ mol), O-(benzotriazol-1-yl)-N,N,N',N'-tetramethyluronium hexafluorophosphate (HBTU; 3.4 mg, 9 μ mol), and 1-hydroxy-1H-benzotriazole (HOBT; 1.4 mg, 10 μ mol) were dissolved in DMF (0.1 mL), and N,N-diisopropylethylamine (DIEA; 3.8 μ L, 22 μ mol) was added. This solution was vortexed and immediately added to the CPG-bound nucleic acid strand. The slurry obtained was stirred for 1 h. The CPG was filtered, washed with DMF (2 \times 1 mL), CH₃CN (2 \times 1 mL), and dried under vacuum (0.01 mbar).

Compound 6a. Yield 30%; HPLC: R_t = 19.8 min; MALDI-TOF MS, negative mode, calculated for C₁₅₅H₁₉₁N₅₁O₇₁P₁₂In [M-H]⁻: m/z 4387.9, found 4386.9.

Compound 6b. Yield 43%; HPLC: R_t = 21.7 min; MALDI-TOF MS, negative mode, calculated for C₁₅₅H₁₉₁N₅₁O₇₁P₁₂Pd [M-H]⁻: m/z 4378.9, found 4381.5.

Compound 6c. Yield 35%; HPLC: R_t = 21.1 min; MALDI-TOF MS, negative mode, calculated for C₁₅₅H₁₉₁N₅₁O₇₁P₁₂Zn [M-H]⁻: m/z 4336.9, found 4338.6.

Compound 6d. Yield 55%; HPLC: R_t = 22.2 min; MALDI-TOF MS, negative mode, calculated for C₁₅₅H₁₉₁N₅₁O₇₁P₁₂Ni [M-H]⁻: m/z 4330.9, found 4331.9.

Compound 12a. Yield 22%; HPLC: R_t = 21.4 min; MALDI-TOF MS, negative mode, calculated for C₂₃₈H₂₉₃N₇₉O₁₂₇P₂₀In [M-H]⁻: m/z 7022.3, found 7024.9.

Compound 12b. Yield 41%; HPLC: R_t = 22.2 min; MALDI-TOF MS, negative mode, calculated for C₂₃₈H₂₉₃N₇₉O₁₂₇P₂₀Pd [M-H]⁻: m/z 7013.3, found 7015.9.

Compound 12c. Yield 25%; HPLC: R_t = 21.7 min; MALDI-TOF MS, negative mode, calculated for C₂₃₈H₂₉₃N₇₉O₁₂₇P₂₀Zn [M-H]⁻: m/z 6971.3, found 6970.6.

Assembly of Oligonucleotide Duplexes. Solutions containing metal complex~ODN conjugates of desired concentrations (0.3–2 μ M) were prepared in phosphate buffer (100 mM, pH 7.0). The mixtures were heated up to 85 °C and then slowly (5 °C/min) cooled

to 22 °C. The duplexes annealed in such a way were used in all further experiments.

Photochemical Reactions. The duplexes prepared as described above with or without the complementary nucleic acid were added to solutions of 1,3-di-(4-carboxyphenyl)-isobenzofuran ($^1\text{O}_2$ trap). The final concentrations of the components of the mixture were as follows: duplexes (0.3 μM), complementary nucleic acid (0.3 μM), $^1\text{O}_2$ trap (300 μM), phosphate buffer (pH 7.0, 100 mM). The mixtures were exposed to the LED-array lamp (672 LED's, 660 nm, Cetoni GmbH) for the definite time periods. The power of the light source was adjusted to provide for 60% conversion of $^1\text{O}_2$ trap in the presence of conjugate **6a** within 30 min (5% of the overall lamp power was used: 1.3 cd at 20 mA). Degradation of the trap was followed by monitoring its absorbance at 46 nm.

■ ASSOCIATED CONTENT

● Supporting Information

HPLC profiles, MALDI-TOF mass spectra of pure metal complex~ODN conjugates, and titration of conjugates **6a** and **6b** with Fmoc-Cys. This material is available free of charge via the Internet at <http://pubs.acs.org>.

■ AUTHOR INFORMATION

Corresponding Author

*Fax: +49-6221-548439. Phone: +49-6221-548441. E-mail: Andriy.Mokhir@urz.uni-heidelberg.de.

■ ACKNOWLEDGMENTS

We thank the Deutsche Forschungsgemeinschaft (DFG MO 1418/1-2 and 1-3) and Ruprecht-Karls-Universität Heidelberg (ZUK49/1 TP 10.10) for financial support.

■ REFERENCES

- (1) Schweitzer, B.; Kingsmore, S. *Curr. Opin. Biotechnol.* **2001**, *12*, 21–27.
- (2) Goldsby, R. A.; Kindt, T. J.; Osborne, B. A.; Kuby, J. *Enzyme-Linked Immunosorbent Assay*. In *Immunology*, 5th ed.; W. H. Freeman: New York, 2003; pp 148–150.
- (3) Selected reviews on nucleic acid dependent catalytic chemical reactions: (a) Kolpachnikov. *Chem. Rev.* **2010**, *110*, 4709–4723. (b) Berger, J.; Oberhuber, M. *Chem. Biodiversity* **2010**, *7*, 2581–2615. (c) Grossmann, T. N.; Strohbach, A.; Seitz, O. *ChemBioChem* **2008**, *9*, 2185–2192. (d) Jacobsen, M. F.; Cló, E.; Mokhir, A.; Gothelf, K. V. *ChemMedChem* **2007**, *2*, 793–799. (e) Silverman, A. P.; Kool, E. *Chem. Rev.* **2006**, *106*, 3775–3789. (f) Liu, D. R.; Li, X. *Angew. Chem., Int. Ed.* **2004**, *43*, 4848–4870.
- (4) (a) Cai, J.; Li, X.; Taylor, J. S. *Org. Lett.* **2005**, *7*, 751–754. Ma, Z.; Taylor, J. S. *Bioconjugate Chem.* **2003**, *14*, 679–683. (b) Ma, Z.; Taylor, J. S. *Bioorg. Med. Chem.* **2001**, *9*, 2501–2510. (c) Ma, Z. C.; Taylor, J. S. *Proc. Natl. Acad. Sci. U.S.A.* **2000**, *97*, 11159–11163.
- (5) (a) Kovács, J.; Mokhir, A. *Bioorg. Med. Chem. Lett.* **2008**, *18*, 5722–5724. (b) Boll, I.; Jentzsch, E.; Kraemer, R.; Mokhir, A. *Chem. Commun.* **2006**, 3447–3449. (c) Boll, I.; Kraemer, R.; Brunner, J.; Mokhir, A. *J. Am. Chem. Soc.* **2005**, *127* (21), 7849–7856. (d) Brunner, J.; Mokhir, A.; Kraemer, R. *J. Am. Chem. Soc.* **2003**, *125* (41), 12410–12411.
- (6) (a) Jentzsch, E.; Mokhir, A. *Inorg. Chem.* **2009**, *48*, 9593–9595. (b) Xu, Y.; Suzuki, Y.; Komiyama, M. *Angew. Chem., Int. Ed.* **2009**, *48*, 3281–3284. (c) Kumar, R.; El-Sagheer, A.; Tumpene, J.; Lincoln, P.; Wilhelmsson, L. M.; Brown, T. *J. Am. Chem. Soc.* **2007**, *129*, 6859–6864.
- (7) (a) Gothelf, K. V.; Brown, R. S. *Chem.—Eur. J.* **2005**, *11*, 1062–1069, and references cited therein. (b) Czapinski, J. L.; Sheppard, T. L. *J. Am. Chem. Soc.* **2001**, *123*, 8618–8619.
- (8) (a) Franzini, R. M.; Kool, E. T. *Chem.—Eur. J.* **2011**, *17*, 2168–2175. (b) Franzini, R. M.; Kool, E. T. *J. Am. Chem. Soc.* **2009**, *131*, 16021–16023. (c) Franzini, R. M.; Kool, E. T. *ChemBioChem* **2008**, *9*, 2981–2988. (d) Furukawa, K.; Abe, H.; Wang, J.; Uda, M.; Koshino, H.; Tsuneda, S.; Ito, Y. *Org. Biomol. Chem.* **2009**, *7*, 671–677. (e) Pianowski, Z.; Gorska, K.; Oswald, L.; Merten, C. A.; Winssinger, N. *J. Am. Chem. Soc.* **2009**, *131*, 6492–6497. (f) Abe, H.; Wang, J.; Furukawa, K.; Oki, K.; Uda, M.; Tsuneda, S.; Ito, Y. *Bioconjugate Chem.* **2008**, *19*, 1219–1226. (g) Pianowski, Z. L.; Winssinger, N. *Chem. Commun.* **2007**, *37*, 3820–3822. (h) Cai, J.; Li, X.; Yue, X.; Taylor, J. S. *J. Am. Chem. Soc.* **2004**, *126*, 16324–16325.
- (9) (a) Miller, G. P.; Silverman, A. P.; Kool, E. T. *Bioorg. Med. Chem.* **2008**, *16*, 56–64. (b) Silverman, A. P.; Baron, E. J.; Kool, E. T. *ChemBioChem* **2006**, *7*, 1890–1894. (c) Abe, H.; Kool, E. T. *Proc. Natl. Acad. Sci. U.S.A.* **2006**, *103*, 263–268. (d) Silverman, A. P.; Kool, E. T. *Nucleic Acids Res.* **2005**, *33*, 4978–4986. (e) Sando, S.; Kool, E. T. *J. Am. Chem. Soc.* **2002**, *124*, 2096–2097.
- (10) (a) Grossmann, T. N.; Seitz, O. *Chem.—Eur. J.* **2009**, *15*, 6723–6730. (b) Grossmann, T. N.; Seitz, O. *J. Am. Chem. Soc.* **2006**, *128*, 15596–15597.
- (11) (a) Rozenmann, M. M.; Liu, D. R. *ChemBioChem* **2006**, *7*, 253–256. (b) Gartner, Z. J.; Tse, B. N.; Grubina, R.; Doyon, J. B.; Snyder, T. M.; Liu, D. R. *Science* **2004**, *305*, 1601–1605. (c) Gartner, Z. J.; Kannan, M. W.; Liu, D. R. *Angew. Chem., Int. Ed.* **2002**, *41*, 1796–1800. (d) Gartner, Z. J.; Liu, D. R. *J. Am. Chem. Soc.* **2001**, *123*, 6961–6663.
- (12) Boersma, A. J.; Megens, R. P.; Feringa, B. L.; Roelfes, G. *Chem. Soc. Rev.* **2010**, *39*, 2083–2092.
- (13) Fournier, P.; Fiammengio, R.; Jäschke, A. *Angew. Chem., Int. Ed.* **2009**, *48*, 4426–4429.
- (14) Visible light induced reactions: (a) Dutta, S.; Mokhir, A. *Chem. Commun.* **2011**, *47*, 1243–1245. (b) Arian, D.; Cló, E.; Gothelf, K. V.; Mokhir, A. *Chem.—Eur. J.* **2010**, *16*, 288–295. (c) Fülöp, A.; Peng, X.; Greenberg, M. M.; Mokhir, A. *Chem. Commun.* **2010**, *46*, 5659–5661. UV-light induced reactions, selected publications: (d) Mukae, M.; Ihara, T.; Tabara, M.; Arslan, P.; Jyo, A. *Supramol. Chem.* **2009**, *21*, 292–295, and refs therein. (e) Yoshimura, Y.; Okamura, D.; Ogino, M.; Fujimoto, K. *Org. Lett.* **2006**, *8*, 5049–5051, and refs therein. (f) Liu, J.; Taylor, J.-S. *Nucleic Acids Res.* **1998**, *26*, 3300–3304.
- (15) Endo, M.; Fujitsuka, M.; Majima, T. *J. Org. Chem.* **2008**, *73*, 1106–1112.
- (16) Stephenson, A. W. I.; Bomholt, N.; Partridge, A. C.; Filichev, V. V. *ChemBioChem* **2010**, *11*, 1833–1839.
- (17) Zhou, H.; Johnson, A. T.; Wiest, O.; Zhang, L. *Org. Biomol. Chem.* **2011**, *9*, 2840–2849.
- (18) Chen, Y.; Zheng, X.; Dobhal, M. P.; Gryshuk, A.; Morgan, J.; Dougherty, T. J.; Oseroff, A.; Pandey, R. K. *J. Med. Chem.* **2005**, *48*, 3692–3695.
- (19) (a) Nguyen, T.-N.; Brewer, A.; Stulz, E. *Angew. Chem., Int. Ed.* **2009**, *48*, 1974–1977. (b) Gerasimchuk, N. N.; Mokhir, A. A.; Rodgers, K. R. *Inorg. Chem.* **1998**, *37* (21), 5641–5650.